ӘУЕ КӨЛІГІ ЖӘНЕ ТЕХНОЛОГИЯЛАР
ВОЗДУШНЫЙ ТРАНСПОРТ И ТЕХНОЛОГИИ
AIR TRANSPORT AND TECHNOLOGY

UDC 621.396.963.84: 004.93'1
IRSTI 47.49.29, 50.05.03
https://doi.org/10.53364/24138614_2025_39_4_1

A. Hasanov[1], I. Isgandarov[1], T. Aliyev[1*]
[1]National Aviation Academy, Baku, Azerbaijan

[*]*E-mail: teymour.aliyev@gmail.com*

ANALYSIS AND MODELING OF ADAPTIVE FILTERS TO IMPROVE THE INTERFERENCE IMMUNITY OF SECONDARY RADAR SIGNALS

Abstract. *This paper explores modern techniques to process and enhance the reliability of radar signals amid strong noise and interference typical for the secondary surveillance radar (SSR) band at 1030/1090 MHz. Air-traffic radar systems play a critical role in ensuring safe and efficient airspace management, however, their performance degrades under strong noise and interference typical of the 1030/1090 MHz band. A comprehensive analysis of filtering and adaptive signal processing algorithms was conducted to improve the signal-to-noise ratio, stabilize target response parameters, and lower false detection rates. For objective comparison, both traditional and advanced digital filtering methods were evaluated. Special focus was placed on comparing the Median, Butterworth, and recursive Kalman filters, implemented and tested in MATLAB with synthetic data and simulated radar scenarios. The effects of filter order, bandwidth, adaptation coefficients, and sampling interval on signal reconstruction quality were investigated. Using statistical, correlation, and probabilistic analyses, an enhanced adaptive threshold detection method was developed, which accounts for the non-stationary background noise, temporal signal correlations, amplitude fluctuations, and dynamic interference parameters in real time. Results demonstrate that combining and recursively applying these filters greatly enhances the robustness of secondary radars against random and systematic interference, reduces estimation error variance, and improves radar reliability. The practical significance lies in the potential integration of these methods into intelligent air-traffic management systems, which can enhance interference immunity, aircraft identification accuracy, and overall radar surveillance quality in civil aviation.*

Keywords: *secondary radar, adaptive filtering, Kalman filter, Butterworth filter, median processing, digital signal processing, signal interference, reliability of radar surveillance.*

Introduction.

Modern radar systems operate in highly congested electromagnetic environments, where both external and internal interference significantly distort received echoes and reduce detection accuracy. To address this, digital adaptive filtering techniques are employed to boost the signal-to-noise ratio and minimize interference. This study examines three radar signal filtering methods: the median filter, the Butterworth filter, and the Kalman filter. Each method offers distinct benefits, ranging from suppressing impulsive noise to adaptively correcting random errors. The performance of the median, Butterworth, and Kalman filters was evaluated using MATLAB simulations with synthetic radar scenarios, allowing a controlled assessment of their effects on SNR, noise suppression, and target detectability.

The proposed integrated method offers dynamic noise estimation, automatic tuning of filtering parameters, and adaptive adjustment of the detection threshold in response to changing

observation conditions. This strategy decreases the probability of false alarms and increases the chances of detecting actual targets. MATLAB simulation results demonstrate that the Kalman filter, when paired with the adaptive MAD threshold, achieves the greatest signal-to-noise ratio improvement and the lowest mean-square error among the filters tested, confirming the effectiveness of the radar signal processing system.

The scientific novelty of this work lies in the development of a hybrid cascade filtering architecture that combines median, Butterworth, and adaptive Kalman filters with dynamic noise covariance estimation and MAD-based thresholding. Unlike traditional approaches that apply these filters separately, the proposed method adaptively tunes filter parameters in real time based on interference density in the 1030/1090 MHz band. This enables robust detection under FRUIT and Mode-S/ADS-B garbling conditions. A major contribution is the adaptive threshold detection algorithm that automatically adjusts the detection threshold using the median absolute deviation, accounting for non-stationary noise statistics. This integrated framework increases interference immunity while maintaining target-signal integrity and enabling stable operation under FRUIT- and garbling-dominated scenarios.

Materials and Methods.

In the 1030–1090 MHz frequency range, used for secondary radar, TCAS, and ADS-B, there is notable spectral congestion. The high interrogation density in the 1030/1090 MHz band leads to false replies (FRUIT), overlapping Mode S messages (garbling), and widespread mutual interference among airborne and ground interrogators. These issues lead to amplitude fluctuations, distorted time stamps, and decreased chances of correct message decoding [9, 11–13].

Recent studies demonstrate that modern air-traffic surveillance systems, particularly ADS-B and Mode S, are increasingly exposed to signal-level interference, intentional manipulation, and growing spectrum load in the 1030/1090 MHz band. Research shows that ADS-B channels remain vulnerable to spoofing, ghost-aircraft injection, trajectory modification, and denial-of-service attacks, while the rising density of Mode S interrogations and DAP-based replies significantly increases channel occupancy and contributes to congestion. These trends collectively indicate that the reliability of cooperative surveillance increasingly depends on robust signal-level processing capable of maintaining integrity under dense-traffic conditions. This further reinforces the need for advanced signal-processing techniques, including the filtering approaches investigated in this study [1, 3, 6].

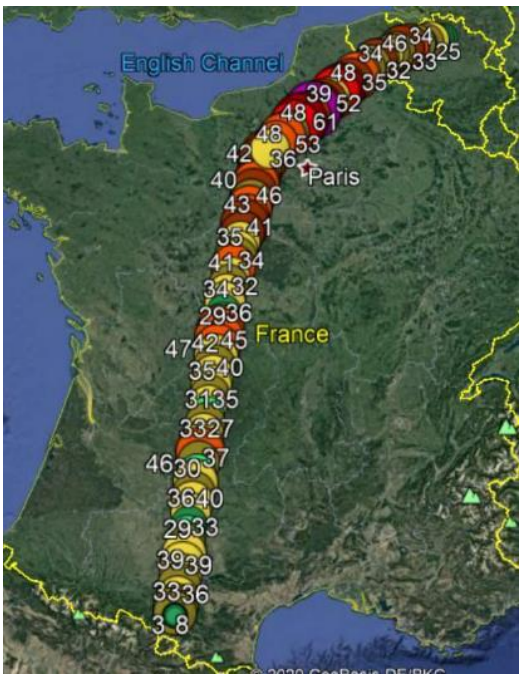

Figure 1 – Number of 1090 MHz signals recorded during flight FR2918

Flight data from flight FR2918, traveling from Barcelona to Brussels on December 16, 2020, indicated heavy congestion on the 1090 MHz frequency band. Overlapping Mode S messages (garbling) and false replies (FRUIT) were identified. These findings reaffirm the ongoing interference issues in the 1090 MHz channel and underscore the importance of adaptive filtering techniques that can dynamically counteract distortions and ensure radar data reliability. The color scale depicts the reception rate of Mode S messages at 1090 MHz, with the highest intensity over northern France, where signal interference and overlap are prevalent under spectral congestion conditions (Figure 1) [14].

In conditions where the 1030/1090 MHz band is overloaded, a combination of filtering techniques—specifically median, Butterworth, and Kalman filters—has been proposed to effectively mitigate various types of interference while maintaining the shape of the desired signals. The median filter, which operates as a nonlinear rank-based method, effectively eliminates impulse outliers without distorting the edges of signals, making it capable of handling signals affected by overlapping noise. The linear Butterworth filter is beneficial for smoothing out high-frequency noise thanks to its maximally flat amplitude-frequency response, and it is commonly utilized in the spectral processing of radar signals. Its straightforward design and reliability are key in reducing background noise. Meanwhile, the Kalman filter is used for recursive optimal state estimation, merging a priori models with incoming measurements. This cascade of filtering techniques results in a high signal-to-noise ratio, decreases the occurrence of false replies (FRUIT), and enhances the overall reliability of real-time radar surveillance [5, 10].

A comparable principle of parallel frequency–time decomposition has been successfully implemented in acousto-optic systems utilizing Bragg diffraction. In such systems, each Bragg angle corresponds to a distinct frequency sub-band, and multichannel reception is achieved by spatially distributing optical beams across a photoelastic medium. This physical analogy aligns with the sub-band decomposition and multichannel filtering approach employed in our deep learning model, where convolutional kernels act as adaptive band-pass filters that isolate overlapping SSR pulses under interference conditions [4, 15].

The combined use of these three filters creates a multi-layered intelligent filtering system, with each method addressing the limitations of the others. To assess filter effectiveness, a synthetic radar signal was produced in MATLAB with added Gaussian noise. Subsequently, median, Butterworth, and Kalman filters were applied for comparison using the radar equation (1) [8].

At the initial stage, the main radar parameters were defined as follows:

- Transmitted power (Pt): 10 kW — the radar's output power indicating the strength of the emitted signal.
- Antenna gain (G): 30 dB — how effectively the antenna transmits and receives signals.
- Wavelength (λ): 0.03 m — corresponding to the radar operating frequency.
- Radar cross section (RCS): 100 m^2 — the effective area describing how strongly the target reflects radar signals.
- Range vector (R): from 1 m to 50 km — a distance array divided into 1000 points for simulation.
- Noise power (NoisePower): 5 μW — representing the random background noise level.
- Sampling frequency (Fs): 10 kHz — the rate at which the signal is sampled, determining temporal resolution.
- Signal length: 1000 samples — the number of discrete time samples in the simulated echo.
- Noise model: zero-mean Gaussian noise with variance corresponding to the specified noise power.

Performance metrics: SNR improvement, mean-square error (MSE) reduction, detection probability and false alarm rate were measured to evaluate filter effectiveness.After setting these parameters, the received signal power is modeled using the classical radar equation, which includes transmitted power, antenna gain, wavelength, radar cross-section, and range. The array

Pr shows the received power at different distances, demonstrating how the signal diminishes with increasing distance, adhering to the inverse fourth-power law ($1/R^4$) due to the double propagation loss—both signal travel to the target and back [7].

$$P_r = \frac{P_t G^2 \lambda^2 \sigma}{(4\pi)^3 R^4} \quad (1)$$

After defining the radar parameters, the received signal power Pr was computed numerically using the classical radar equation (1). For each value in the range vector R, a corresponding power sample was generated, forming a one-dimensional array that represents how signal strength decreases with distance. To emulate realistic operating conditions, zero-mean Gaussian noise with power NoisePower was added to the theoretical signal, producing a noisy received signal according to expression (2). All calculations were performed in MATLAB using predefined parameters and mathematical models. This numerical approach ensured a consistent simulation of the signal behavior required for subsequent filtering and comparative analysis.

$$\text{ReceivedSignal} = \text{Pr} + \text{NoisePower} \cdot \text{randn}(\text{size}(\text{Pr})) \quad (2)$$

To process the noisy radar signal, several filtering techniques were applied sequentially. First, a matched filter was used to enhance the signal-to-noise ratio by correlating the received signal with a known reference waveform. This step emphasizes components of the signal that correspond to the expected pulse shape. Next, a median filter was employed to reduce impulsive noise and suppress narrow, high-amplitude fluctuations caused by interference. The median filter replaces each sample with the median value of its local neighborhood, improving robustness to outliers.

To further smooth the signal and suppress high-frequency noise, a Butterworth low-pass filter was applied. This filter provides a maximally flat frequency response in the passband, preserving the main structure of the radar echo while attenuating rapid fluctuations. Finally, an adaptive Kalman filter was used to dynamically estimate the true signal in the presence of noise. The Kalman filter predicts the next signal state based on a linear system model and continuously adjusts its estimates using incoming measurements [2].

This approach is particularly effective for modeling smooth radar returns, gradual range variations, and target motion. Proposed step-by-step implementation forms the foundation of an adaptive cascade filtering system, where each method performs a distinct role: the matched filter enhances useful echoes, the median filter removes impulsive distortions, and the Kalman filter adaptively stabilizes the signal and compensates for noise variations in real time [2, 7].

The adaptive Kalman filter processes the radar signal in two main stages: prediction and update. During the prediction stage, the filter estimates the next state of the signal and the associated uncertainty using equations (5) and (6). This step forecasts the expected signal dynamics before receiving new measurements.In the update stage, the filter adjusts the predicted state based on the incoming noisy measurement. The Kalman gain, calculated using equation (7), controls how strongly the new measurement influences the state estimate. A higher gain increases sensitivity to new data, while a lower gain emphasizes the predicted state. To maintain adaptability under fluctuating interference levels, the process noise covariance Q is continuously recalculated using expression (3). This enables the filter to adjust its noise model in real time, particularly under conditions where overlapping ADS-B and Mode S signals create rapidly changing interference patterns. As a result, the adaptive Kalman filter dynamically balances prediction and measurement information, providing a stable and accurate estimate of the radar signal.

The Kalman filter operates through sequential prediction and measurement-based correction of the signal state. The input data is stored in the *ReceivedSignal* array, which contains discrete

samples of the radar signal received. To maintain the filter's adaptability, the covariances of process and measurement noise are computed dynamically based on the signal's features. To enhance the algorithm's stability, an adaptive estimation of noise parameters is implemented. The process noise covariance is calculated using a specific formula that defines the adaptive parameter Q, which represents the process covariance in the Kalman filter. This approach allows the Kalman filter parameters to be automatically adjusted as the noise level varies, especially when overlapping ADS-B and Mode S messages occur. Consequently, the system continuously fine-tunes its sensitivity to noise and updates the weighting of new measurements.

$$Q = max\left(\frac{1}{2}var(ReceivedSignal[max(1, k - 10): k]), 10^{-6}\right) \quad (3)$$

During the adaptive adjustment of the process and measurement noise covariances, a sliding window of the last 10 measurements is used to dynamically estimate the noise level in the signal. The minimum value of 10^{-6} prevents the covariance from becoming zero, which could lead to filter instability. The measurement noise covariance is calculated using the following formula:

$$R_{kalman} = NoisePower \times 1.2 \quad (4)$$

where NoisePower is the predefined noise power level. The coefficient 1.2 provides an additional margin to account for measurement uncertainty.

At the prediction stage, the algorithm forecasts the new state of the system:

$$\mathrm{x_{pred}} = \mathrm{A} \cdot \mathrm{x_{est}} \quad (5)$$

$$\mathrm{P_{pred}} = \mathrm{A} \cdot \mathrm{P} \cdot \mathrm{A} + \mathrm{Q} \quad (6)$$

Here:

x_{est} – estimated system state at the previous step;
x_{pred} –predicted state at the next time moment;
A – state transition matrix describing how the system evolves over time;
P – covariance matrix of the estimation error (uncertainty);
$\mathrm{P_{pred}}$– predicted covariance of the estimation error;
Q — process noise covariance, which determines the uncertainty level of the model.

This stage allows predicting the probable target position before obtaining a new measurement. In the 1030–1090 MHz frequency band, equations (5) and (6) describe the prediction of the target's position, velocity, and echo amplitude between successive pulses. The parameter Q, calculated according to equation (3), provides adaptation to changing interference levels, making the filter stable under Mode S/ADS-B channel congestion conditions.

At the update stage, after receiving a new measurement, the state estimate is corrected. For this purpose, the Kalman gain is calculated:

$$\mathrm{K} = \mathrm{P_{pred}} \cdot \mathrm{H}/(\mathrm{H} \cdot \mathrm{P_{pred}} \cdot \mathrm{H} + \mathrm{R_{kalman}}) \quad (7)$$

where:

K — Kalman gain, determining how much the new measurement affects the updated state;
H — observation matrix linking the system state with the measurement;
$\mathrm{R_{kalman}}$ — measurement noise covariance.

This coefficient defines the balance between reliance on the model and the measurement: if the measurement noise is large (high $\mathrm{R_{kalman}}$), the filter trusts the model prediction more; if small, it relies more on measurements. Then the state estimate is updated according to:

$$\mathrm{x_{est}} = x_{\mathrm{pred}} + \mathrm{K} \cdot \left(\mathrm{ReceivedSignal(k)} - \mathrm{H} \cdot x_{\mathrm{pred}}\right) \quad (8)$$

where the difference (ReceivedSignal−H·xpred) is the innovation, i.e., the prediction error. The filter corrects the predicted state by adding a weighted adjustment proportional to this error, scaled by the Kalman gain K. The covariance of the estimation error is also updated as follows:

$$P = (1 - K \cdot H) \cdot P_{pred} \quad (9)$$

After processing each measurement, the corrected state value is stored in the array FilteredSignal_Kalman for further analysis. This array contains the filtered signal values, free from impulse outliers and random noise. After correction, the uncertainty (estimation error) decreases — the filter becomes more confident in its results [2, 7].

To suppress high-frequency noise while preserving the informative low-frequency components of the radar echo, a 5th-order Butterworth low-pass filter was applied. The cutoff frequency Fc was selected to limit the bandwidth of the signal to the physically relevant range, while the sampling frequency Fs determined the normalized cutoff Fc/(Fs/2) used in the digital filter design. The Butterworth filter provides a maximally flat response in the passband, ensuring smooth signal shaping and minimizing amplitude distortions. After computing the filter coefficients using expression (10), the filter was applied to the received signal according to equation (11), producing a smoothed version of the radar echo suitable for subsequent threshold-based detection.

A 5th-order Butterworth low-pass filter was then applied to attenuate high-frequency components while preserving the main structure of the radar echo. The filter was configured with a cutoff frequency Fc = 2000 Hz and a sampling frequency Fs = 10 kHz, which determine the normalized cutoff Fc/(Fs/2) used in the digital filter design. A 5th-order filter was selected to ensure a smooth passband response and a sufficiently steep roll-off beyond the cutoff frequency.

After computing the filter coefficients according to expression (10), the filter was applied to the received signal using the digital filtering equation (11). This approach effectively reduces high-frequency noise and improves the signal-to-noise ratio (SNR) without introducing significant distortion. Compared with other filtering techniques, the Butterworth filter provides a maximally flat amplitude response in the passband, making it a reliable tool for preprocessing radar data prior to target detection.

Before applying the filter, its coefficients b and a were computed using the standard design expression:

$$[b, a] = \text{Butterworth}(n = 5, fc/(Fs/2)) \quad (10)$$

In this expression, the first argument defines the filter order (n = 5), while the second argument represents the normalized cutoff frequency Fc/(Fs/2), computed relative to the Nyquist frequency. Since a low-pass response is required, the filter is designed to attenuate all components above the cutoff frequency Fc.

After calculating the coefficients, the filter is applied to the received signal ReceivedSignal using the digital filtering equation:

$$\text{FilteredSignalButterworth} = \text{filter}(b, a, \text{ReceivedSignal}) \quad (11)$$

Applying this filtering method effectively suppresses high-frequency noise, improving the signal-to-noise ratio (SNR) without significant distortion of the useful signal. Unlike many other methods, the Butterworth filter provides a smooth frequency response, minimizing phase distortion. The obtained results demonstrate that the proposed method is an effective tool for preprocessing radar data before further analysis.

Adaptive threshold-based target detection in radar signals.

Target detection in radar systems is a complex task, especially in the presence of noise and interference. The detection process is based on comparing the filtered signal with a threshold value that is dynamically calculated considering the statistical characteristics of the signal.

The adaptive threshold (THRESHOLD) is determined using the Median Absolute Deviation (MAD), which allows the algorithm to take into account the variability of noise in the signal:

$$MAD = \text{median}(|\ \text{FilteredSignalKalman} - \text{median}(\text{FilteredSignalKalman})\ |) \times 1.4826 \quad (12)$$

Then, the detection threshold is calculated as:

$$\text{Threshold} = \text{median}(\text{FilteredSignalKalman}) + 2 \times \text{MAD} \quad (13)$$

Target detection is performed by comparing the filtered signal with the adaptive threshold. A detection is registered when the signal amplitude exceeds the threshold value, and no target is declared otherwise. This procedure produces a binary detection sequence, where samples above the threshold correspond to potential target returns.

Figure 2 illustrates the points in space where the system detects the presence of a useful signal (detection) and where the signal is absent. The X-axis (Range, m) shows the distance to the target or the observed area, while the Y-axis (Detection Status) represents the detection state. The value 1 indicates a detected signal, while 0 denotes no detection. The red vertical lines on the graph mark the moments when the system registered signal detection.

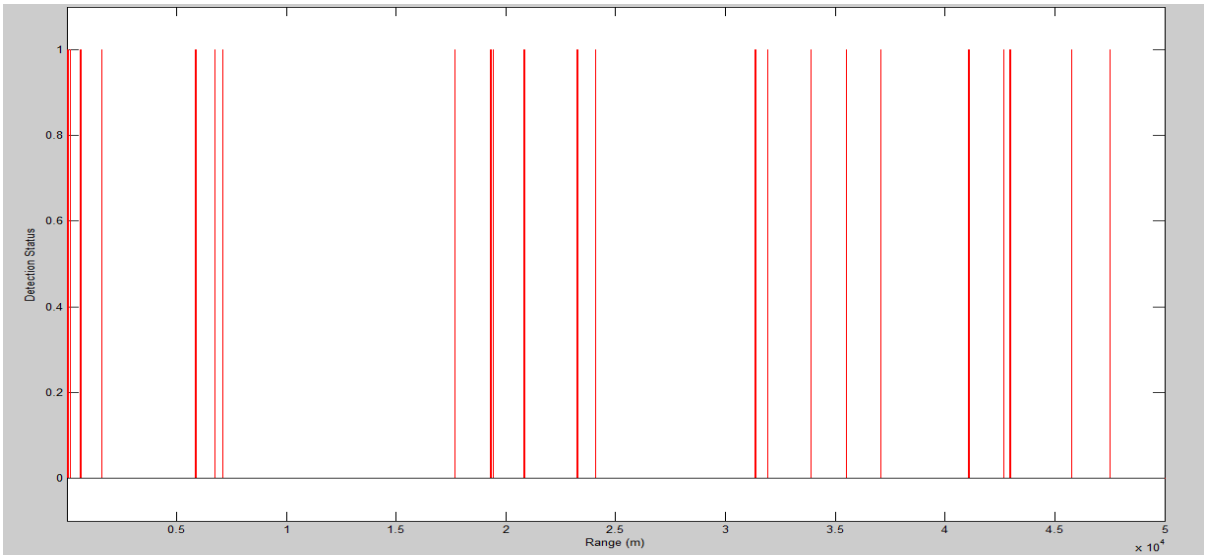

Figure 2 – Signal detections using adaptive Kalman filtering *(Signal detections using adaptive Kalman filtering. The X-axis represents the range in meters, and the Y-axis shows the detection status (1 – target detected, 0 – no detection). Red vertical lines mark detection events)*

The analysis of the graph shows that rare and narrow peaks correspond to the effective noise suppression by the Kalman filter, which allows identifying only significant signals. The filtering process eliminates false detections caused by noise in the raw data. Individual detection moments (red lines) may correspond to real reflected signals or objects.

Thus, the Kalman filter helps reduce the number of false alarms by adaptively suppressing noise. The graph confirms that the signal processing enables selective target detection compared to the original noisy data. To increase detection accuracy, the detection threshold can be adjusted in the MATLAB code via the Median Absolute Deviation (MAD) parameter. This approach ensures reliable signal detection even in complex environments with high noise and fluctuation levels [2].

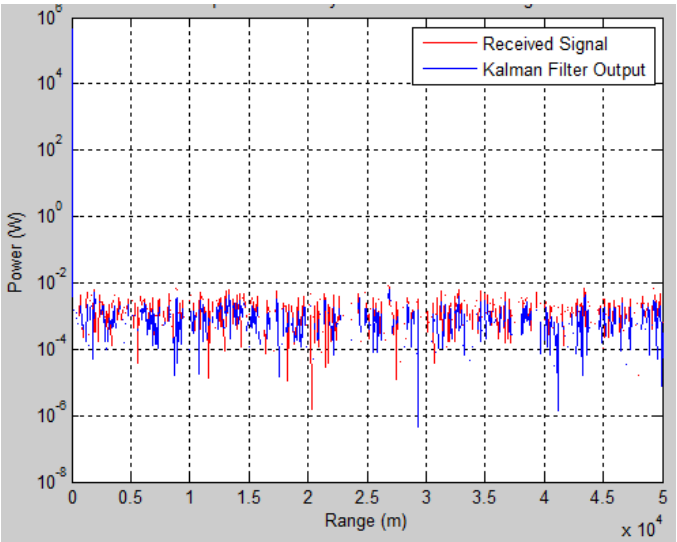

Figure 3 – Comparison of the noisy input radar signal (Received Signal) and the filtered signal after Kalman filter processing (Kalman Filter Output) in MATLAB (The X-axis shows range in meters (0–50 000 m), and the Y-axis shows signal power on a logarithmic scale, illustrating noise suppression)

The red line in Figure 3 represents the original radar signal with added Gaussian noise, while the blue line shows the signal processed by the Kalman filter. The X-axis indicates the range from the radar to the target (in meters), covering the interval from 0 to 50,000 meters. The Y-axis displays the signal power on a logarithmic scale, allowing better visualization of both weak and strong echoes.

The comparison of the two signals shows that the red “Received Signal” experiences significant amplitude fluctuations caused by noise. The power level changes chaotically with range, complicating interpretation. In contrast, the blue “Kalman Filter Output” signal has a smoothed profile and more accurately follows the expected variations in power without abrupt jumps. This confirms the efficiency of the Kalman filter in noise suppression and signal restoration.

The Kalman filter demonstrates a high ability to remove noise while preserving useful information. The difference between the red and blue curves reflects the degree of noise suppression, which is particularly important in radar systems that must detect weak targets in the presence of interference. The graph clearly shows that the Kalman filter significantly improves signal quality, reduces the influence of random fluctuations, and preserves the underlying signal structure. In radar applications, where measurement precision is crucial, such processing enhances the reliability and accuracy of target detection.

Results and Discussion.

The filtering methods were quantitatively evaluated using two metrics: improvements in signal-to-noise ratio (SNR) and reductions in mean-square error (MSE). The analysis was performed using a Monte-Carlo simulation with 50 independent runs to ensure statistical stability of the results. The clean reference signal was generated according to the radar equation, and noise-corrupted data were processed by each filtering method. Figure 4 and Table 1 summarizes the simulation results.

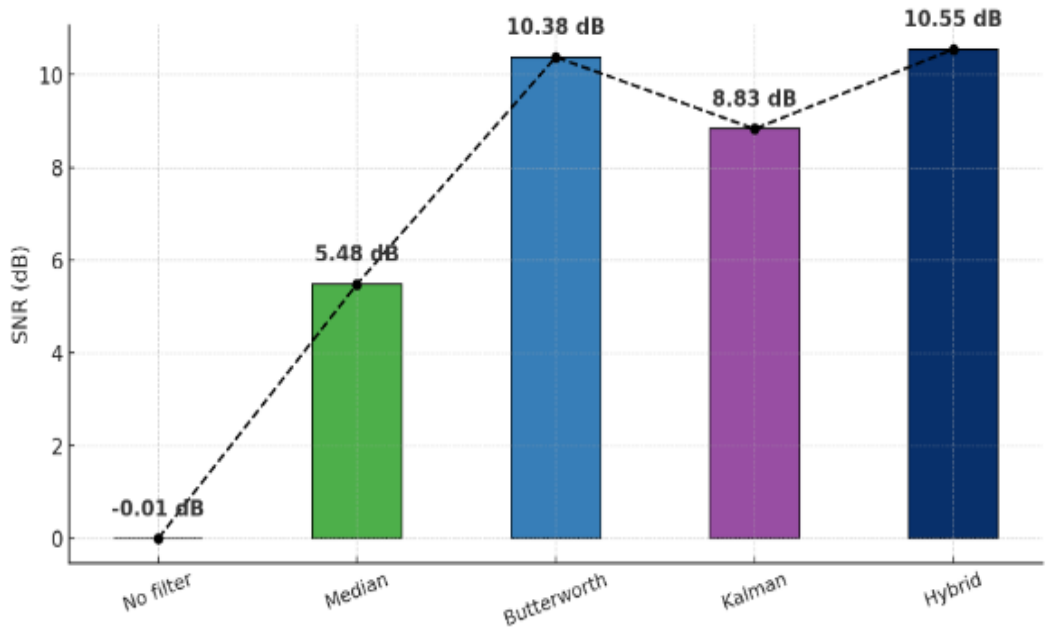

Figure 4 – Improvement of SNR for Different Filtering Methods

The median filter yields a moderate SNR increase by removing impulsive outliers, though its smoothing effect limits accuracy in some cases. The Butterworth filter achieves a significantly better SNR (>10 dB) by attenuating high-frequency components. The adaptive Kalman filter yields unbiased minimum-variance estimates but remains sensitive to changes in the noise covariance. The proposed hybrid cascade achieves the best performance in both metrics due to the complementary nature of its components: the median filter suppresses outliers, the Butterworth filter removes broadband noise, and the Kalman filter refines the final estimate (table 1).

Table 1 – Quantitative Performance Comparison of Radar Signal Filtering Methods

Filtering Method	SNR (dB)	MSE	SNR Improvement (ΔSNR)
No filtering	–0.01 dB	1.0023	–
Median filter	5.48 dB	0.2842	+5.48 dB
Butterworth filter (low-pass, 5th order)	10.38 dB	0.0924	+10.38 dB
Adaptive Kalman filter	8.83 dB	0.1318	+8.84 dB
Hybrid cascade (median + Butterworth + Kalman)	10.55 dB	0.0895	+10.56 dB

In the baseline case without filtering, the input SNR was approximately 0 dB, meaning that the signal power was nearly equal to the noise power and the radar echo was heavily distorted. After applying the proposed filtering methods, the SNR increased by about 5–10 dB, while the MSE decreased by almost an order of magnitude, indicating a substantial improvement in signal quality. The bar charts (Figure 4) visualize the SNR enhancement achieved by each filtering technique, demonstrating that the hybrid cascade filter provides the highest gain. This combined approach, with an SNR of 10.55 dB and MSE 0.0895, outperforms individual median (SNR: 5.48 dB; MSE: 0.2842), Butterworth (SNR: 10.38 dB; MSE: 0.0924), and Kalman filters (8.83 dB; MSE: 0.1318), confirming its effectiveness in suppressing noise and enhancing radar signal reliability.

Conclusion.

The study presents an analysis and modeling of adaptive radar signal filtering methods in the 1030–1090 MHz frequency band, which is typical for secondary surveillance radar, TCAS, and ADS-B systems. The research has shown that the use of a combination of median, Butterworth, and Kalman filters significantly improves signal processing reliability and reduces the influence

of both random and correlated noise. Simulation results confirm that median filtering effectively suppresses impulsive distortions, the Butterworth filter provides broadband noise reduction, and the adaptive Kalman filter delivers the lowest estimation error. Their combined use significantly strengthens interference immunity in the congested 1030–1090 MHz band. The implementation of adaptive threshold detection based on Median Absolute Deviation (MAD) allows creating a dynamically adjustable detection criterion sensitive to variations in the interference environment. This ensures the stable operation of the radar system under 1090 MHz frequency channel congestion and maintains data reliability even under overlapping Mode S and ADS-B transmissions.

References

1. Abu Al-Haija, Q., & Al-Tamimi, A. (2024). Secure aviation control through a streamlined ADS-B perception system. Applied System Innovation, 7(2), 27. https://doi.org/10.3390/asi7020027

2. Barton, D. K. (2013). Radar equations for modern radar. Artech House.

3. Ceballos-Gutiierrez, J., Aranda-Escolástico, E., & Moreno-Salinas, D. (2025). Optimisation of spectrum use by Mode S surveillance systems through coordinated DAP extraction. IEEE Aerospace and Electronic Systems Magazine. https://doi.org/10.1109/MAES.2024.3482293

4. Hasanov, A. R., Hasanov, R. A., & Rustamov, A. R. (2018). Mathematical modeling of characteristics of an acousto-optic delay line and evaluation of their adequacy. Instruments and Experimental Techniques, 61(3), 411–417. https://doi.org/10.1134/S0020441218030119

5. Karl, W. C., Leeb, S. B., Jones, L. A., & Verghese, G. C. (1992). Applications of rank-based filters in power electronics. IEEE Transactions on Power Electronics, 7(3), 437–447. https://doi.org/10.1109/63.145140

6. Olive, X., Krummen, J., Figuet, B., & Alligier, R. (2024). Filtering techniques for ADS-B trajectory preprocessing. Journal of Open Aviation Science, 2, 1–18. https://doi.org/10.59490/joas.2024.7882

7. Skolnik, M. I. (1980). Introduction to radar systems (2nd ed.). McGraw-Hill

8. Song, F., Li, Y., Cheng, W., Dong, L., Li, M., & Liu, J. (2022). An improved Kalman filter based on long short-memory recurrent neural network for nonlinear radar target tracking. Wireless Communications and Mobile Computing, 2022, Article 5020443. https://doi.org/10.1155/2022/5020443

9. Aliyev, T. R., & Isgandarov, I. A. (2025). Enhancing ATC radar system reliability: Strategies and modern solutions. International Journal of Aviation Science and Technology, 6(1), 45–58. https://doi.org/10.23890/IJAST.vm06is01.0105

10. Wang, B. (2024). Signal processing based on Butterworth filter: Properties, design, and applications. Highlights in Science, Engineering and Technology, 97, 72–78

11. Isgandarov, I. A., & Aliyev, T. R. (2024). Review of innovative methods to improve the reliability of radar information in air traffic control. Bulletin of Civil Aviation Academy, 3(34), 77–88. https://doi.org/10.53364/24138614_2024_34_3_6

12. Isgandarov, I. A., & Aliyev, T. R. (2023). Development of a model of the TCAS autonomous diagnostic system using non-contact current sensors. In T. H. Karakoc, A. Yilmaz, & A. Türk (Eds.), Novel techniques in maintenance, repair, and overhaul (pp. 117–121). Springer. https://doi.org/10.1007/978-3-031-42041-2_16

13. Isgandarov, I. A., & Aliyev, T. R. (2024). Development of prospective methods for increasing the reliability of radar information in the ATC system. In T. H. Karakoc et al. (Eds.), Research and updates on the use of artificial intelligence in drone technology: ISUDEF 2024 (pp. 240–246). Springer. https://doi.org/10.1007/978-3-032-07678-6_43

14. Borin Kaduk Aguilar. (2021). Analysis and optimisation of radio spectrum pollution on 1030/1090 MHz bands associated with Mode S transponders (Bachelor thesis). Universitat Politècnica de Catalunya

15. Hasanov, A. R., Hasanov, R. A., Rustamov, A. R., Ahmadov, R. A., Suleymanov, I. I., & Sadikhov, M. V. (2022). Acousto-optic spectral-time analyzer. Applied Physics, 2, 62–71. https://doi.org/10.51368/1996-0948-2022-2-62-71

ЕКІНШІЛІК РАДИОЛОКАЦИЯ СИГНАЛДАРЫНЫҢ КЕДЕРГІГЕ ТӨЗІМДІЛІГІН АРТТЫРУ ҮШІН АДАПТИВТІ СҮЗГІЛЕРДІ ТАЛДАУ ЖӘНЕ МОДЕЛЬДЕУ

Аңдатпа. *Бұл мақалада екінші реттік радиолокация диапазонына (1030/1090 МГц) тән күшті шу мен кедергілер жағдайында радиолокациялық сигналдарды өңдеу және олардың сенімділігін арттырудың заманауи тәсілдері қарастырылады. Әуе қозғалысының радарлық жүйелері әуе кеңістігін қауіпсіз және тиімді басқаруды қамтамасыз етуде маңызды рөл атқарады, дегенмен, олардың өнімділігі 1030/1090 МГц диапазонына тән күшті шу мен кедергілер кезінде төмендейді. Зерттеу барысында сигнал/шу қатынасын арттыруға, мақсаттық жауап параметрлерінің тұрақтылығын қамтамасыз етуге және жалған дабыл ықтималдығын азайтуға бағытталған сүзгілеу мен бейімделген сигналдық өңдеу алгоритмдері егжей-тегжейлі талданды. Объективті салыстыру жүргізу үшін классикалық және жетілдірілген цифрлық сүзгілеу тәсілдері қарастырылды. Әсіресе MATLAB ортасында жүзеге асырылып, синтетикалық деректер мен типтік радиолокациялық сценарийлердің модельдері негізінде сыналған медиандық, Баттерворт және рекурсивті Калман сүзгілерін салыстырмалы зерттеу ерекше назарға алынды. Сүзгінің реті, өткізу жолағы, бейімделу коэффициенттері мен дискреттеу қадамының сигналды қалпына келтіру сапасына әсері зерттелді. Статистикалық, корреляциялық және ықтималдық талдау нәтижесінде фондық шудың бейстационарлы табиғатын, сигналдар арасындағы уақытша корреляцияны және амплитудалық тербелістерді ескеретін бейімделген табалдырықтық анықтау әдісі жетілдірілді. Алынған нәтижелер біріктірілген және рекурсивті сүзгілерді қолдану екінші реттік радиолокаторлардың кездейсоқ және жүйелік кедергілерге төзімділігін едәуір арттыратынын, бағалау қателіктерінің дисперсиясын азайтатынын және радиолокациялық ақпараттың сенімділігін жоғарылататынын көрсетті. Зерттеудің практикалық құндылығы — ұсынылған әдістерді азаматтық авиацияның интеллектуалды әуе қозғалысын басқару және радиолокациялық бақылау жүйелеріне енгізу арқылы кедергіге төзімділікті, ұшақтарды сәйкестендіру дәлдігін және радиолокациялық бақылау сапасын арттыру мүмкіндігімен айқындалады.*

Түйін сөздер*: екінші реттік радиолокация, бейімделген сүзгілеу, Калман сүзгісі, Баттерворт сүзгісі, медиандық өңдеу, цифрлық сигналдарды өңдеу, сигналдардың интерференциясы, радиолокациялық бақылаудың сенімділігі.*

АНАЛИЗ И МОДЕЛИРОВАНИЕ АДАПТИВНЫХ ФИЛЬТРОВ ДЛЯ ПОВЫШЕНИЯ ПОМЕХОУСТОЙЧИВОСТИ СИГНАЛОВ ВТОРИЧНОЙ РАДИОЛОКАЦИИ

Аннотация. *В данной статье рассматриваются современные подходы к обработке и повышению достоверности радиолокационных сигналов в условиях сильных шумовых и помеховых воздействий, характерных для диапазона вторичной радиолокации (1030/1090 МГц). Системы радиолокационного контроля воздушного движения играют важнейшую роль в обеспечении безопасного и эффективного управления воздушным пространством, однако их производительность снижается в условиях сильного шума и помех, типичных для диапазона 1030/1090 МГц. В работе проведён детальный анализ алгоритмов фильтрации и адаптивной обработки радиолокационных сигналов, направленных на повышение отношения сигнал/шум, стабилизацию параметров целевых откликов и уменьшение вероятности ложных срабатываний при регистрации отметок. Для более*

объективного сравнения рассмотрены как классические, так и усовершенствованные подходы цифровой фильтрации. Особое внимание уделено сравнительному исследованию медианного фильтра, фильтра Баттерворта и рекурсивного фильтра Калмана, реализованных и протестированных в среде MATLAB с использованием синтетически сгенерированных данных и имитационных моделей типичных радиолокационных сценариев. При этом исследовались влияние порядка фильтра, полосы пропускания, коэффициентов адаптации и временного шага дискретизации на качество восстановления сигнала. На основе статистического, корреляционного и вероятностного анализа предложен усовершенствованный метод адаптивного порогового обнаружения целей. Полученные результаты подтверждают, что потенциальное использование комбинированных и рекурсивных фильтров позволяет значительно повысить устойчивость вторичных радиолокаторов к случайным и системным помехам, снизить дисперсию ошибок оценки и повысить достоверность радиолокационной информации. Практическая ценность работы заключается в возможности внедрения предложенных методов в интеллектуальные системы обработки данных управления воздушным движением для повышения помехоустойчивости, точности идентификации воздушных судов и улучшения качества радарного наблюдения в гражданской авиации.

Ключевые слова: *вторичная радиолокация, адаптивная фильтрация, фильтр Калмана, фильтр Баттерворта, медианная обработка, цифровая обработка сигналов, интерференция сигналов, достоверность радиолокационного наблюдения.*

Information about the authors

Afig Hasanov	Doctor of Technical Sciences, Professor. National Aviation Academy, Azerbaijan, Baku. E-mail: ahesenov@naa.edu.az
Islam Isgandarov	PhD, Professor, Head of Department at the National Aviation Academy, Azerbaijan, Baku E-mail: iisgandarov@naa.edu.az
Teymur Aliyev	Doctoral candidate. National Aviation Academy. Azerbaijan, Baku. E-mail: teymour.aliyev@gmail.com

Сведения об авторах

Афиг Гасанов	доктор технических наук, профессор. Национальная авиационная академия, Азербайджан, Баку. E-mail: ahesenov@naa.edu.az
Ислам Искендеров	Доктор технических наук, профессор, заведующий кафедрой Национальной авиационной академии, Азербайджан, Баку E-mail: iisgandarov@naa.edu.az
Теймур Алиев	Докторант Национальной авиационной академии, Азербайджан, Баку, E-mail: teymour.aliyev@gmail.com

Авторлар туралы мәлімет

Афиг Гасанов	техника ғылымдарының докторы, профессор. Ұлттық авиация академиясы, Әзірбайжан, Баку. E-mail: ahesenov@naa.edu.az
Ислам Искендеров	PhD, профессор, Ұлттық авиация академиясының кафедра меңгерушісі, Әзербайжан, Баку E-mail: iisgandarov@naa.edu.az
Теймур Алиев	Ұлттық авиация академиясының докторанты, Әзірбайжан, Баку, E-mail: teymour.aliyev@gmail.com

Appendix A

Editor - C:\Program Files\MATLAB\R2014a\bin\Untitled.m

Untitled.m | sss.m

This file can be published to a formatted document. For more information, see the publishing video or help.

```
%% MATLAB Code for Adaptive Radar Signal Filtering and Analysis

% 1. Define radar parameters
Pt = 1e4; % Increased transmitted power (W)
G = 30; % Antenna gain (dB)
Lambda = 0.03; % Wavelength (m)
RCS = 100; % Radar Cross Section (m^2)
R = linspace(1, 50e3, 1000); % Reduced range (m) to better visualize sign
NoisePower = 5e-6; % Increased Noise power (W) to make noise more visible

% 2. Compute received power using radar equation
Pr = (Pt * (10^(G/10))^2 * Lambda^2 * RCS) ./ ((4 * pi)^3 * R.^4);

% Display signal properties
disp(['Max Pr: ', num2str(max(Pr))]);
disp(['Min Pr: ', num2str(min(Pr))]);
```

Code fragment for calculating received power according to Equation (1)

Editor - C:\Program Files\MATLAB\R2014a\bin\Untitled.m

Untitled.m | sss.m

This file can be published to a formatted document. For more information, see the publishing video or help.

```
% 3. Add Gaussian noise to received signal
ReceivedSignal = Pr + sqrt(NoisePower) * randn(size(Pr));

% 4. Adaptive filtering techniques

% Matched filter (correlation with expected signal)
filter_coeff = fliplr(Pr); % Matched filter based on transmitted signal
MatchedFilteredSignal = conv(ReceivedSignal, filter_coeff, 'same');

% Median filter to avoid over-smoothing
n = 5; % Filter order
FilteredSignal_Median = medfilt1(ReceivedSignal, n);

% Adaptive Kalman Filter
A = 1; % System dynamics coefficient
H = 1; % Measurement matrix
x_est = ReceivedSignal(1); % Initial state estimate
P = 1; % Initial estimate error covariance
FilteredSignal_Kalman = zeros(size(ReceivedSignal));
```

MATLAB code for implementing adaptive radar signal filtering methods: matched, median, and Kalman filters

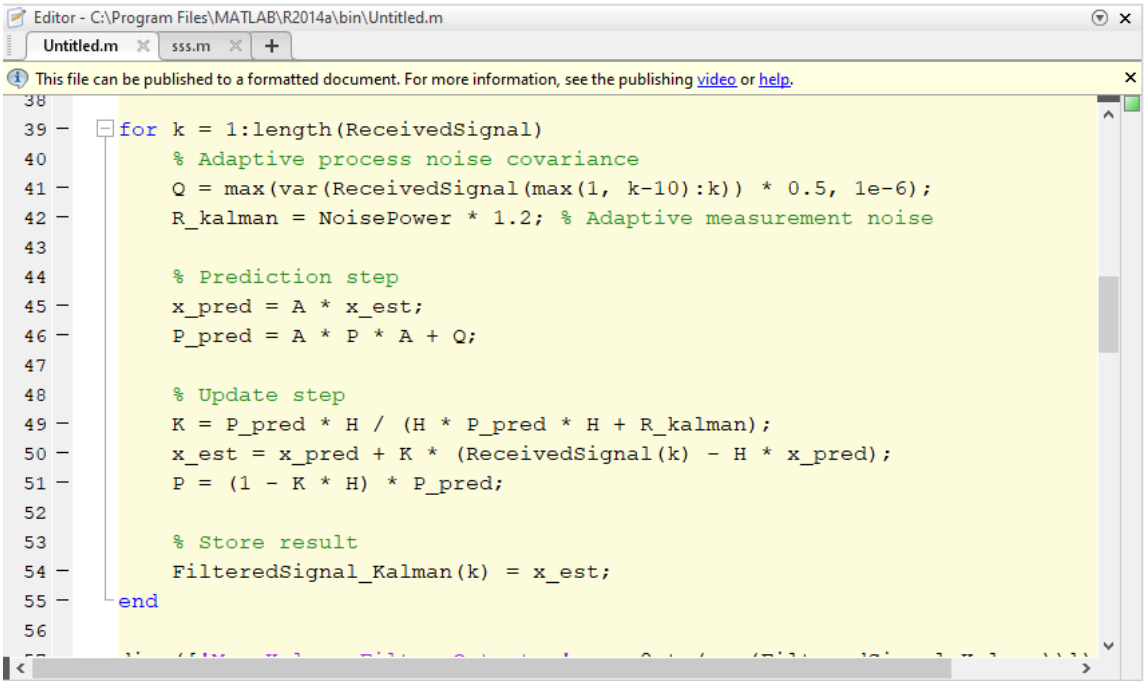

Algorithm of the adaptive Kalman filter

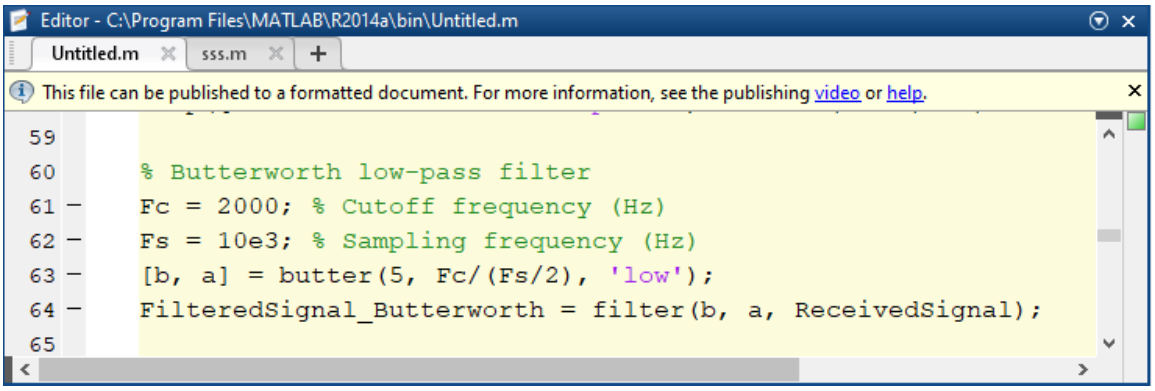

Code for implementing the Butterworth filter to suppress high-frequency noise

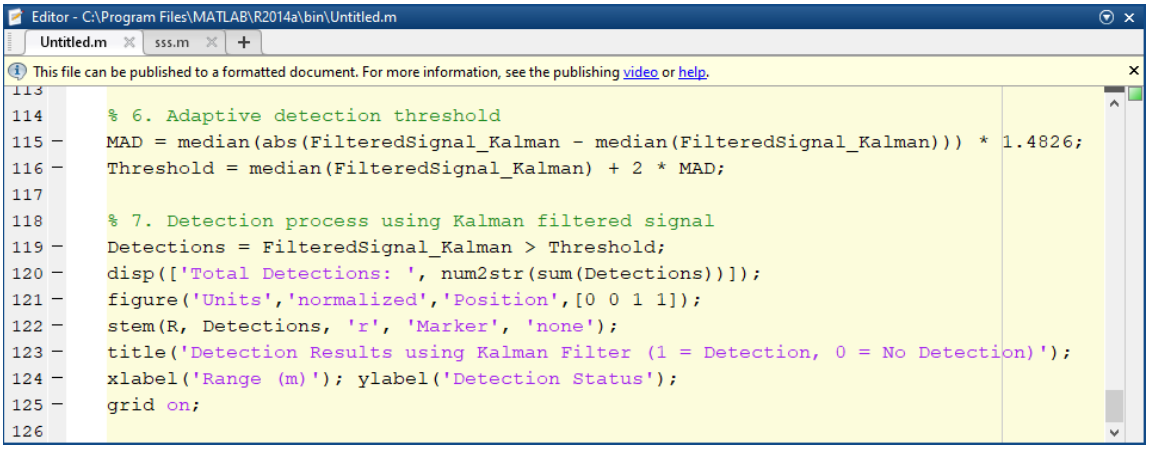

Code for target threshold detection using the Kalman filter